Linear models of activation cascades: analytical solutions and applications

M. Beguerisse-Díaz[a,b], P.J. Ingram[a,c], R. Desikan[b], M. Barahona[a]

[a] *Department of Mathematics, Imperial College London, South Kensington Campus, London, SW7 2AZ, U.K.*
[b] *Department of Life Sciences, Imperial College London, South Kensington Campus, London, SW7 2AZ, U.K.*
[c] *Centre for Integrative Systems Biology at Imperial College, Imperial College London, South Kensington Campus, London, SW7 2AZ, U.K.*

Abstract

Activation cascades are prevalent in cell signalling mechanisms. We study the classic model of linear activation cascades and find that in special but important cases the output of an entire cascade can be represented analytically as a function of the input and a lower incomplete gamma function. We also show that if the inactivation rate of a single component is altered, the change induced at the output is independent of the position in the cascade of the modified component. We use our analytical results to show how one can reduce the number of equations and parameters in ODE models of cell signalling cascades, and how delay differential equation models can sometimes be approximated through the use of simple expressions involving the incomplete gamma function.

Keywords: Activation cascades, linear models, MAPK, gamma function, model reduction, delay differential equations.

1. Introduction

Activation cascades are frequently found in biological signal transduction systems [12, 18]. Perhaps one of the best studied examples is the *mitogen-activated protein kinase* (MAPK) cascade, which plays a central role in im-

Email addresses: m.beguerisse-diaz08@imperial.ac.uk (M. Beguerisse-Díaz), m.barahona@imperial.ac.uk (M. Barahona)

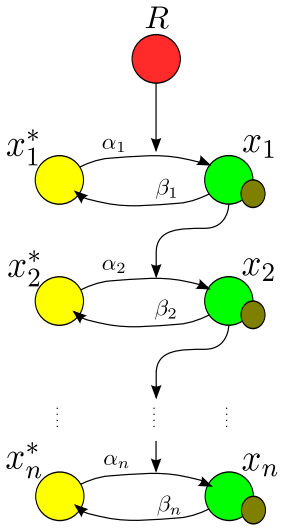

Figure 1: (Colour) A cascade of length n. The nodes in the cascade can either be in an inactive state x_i^*, or active x_i, shown graphically in the nodes of the right by the addition of a phosphate group. An external signal $R(t)$ activates the first node. Once a node is active, it can activate the next node, and so on until the end. The activation rates are α_i and the inactivation rates are β_i. Image adapted from [12].

portant cellular functions such as regulation of the cell cycle, stress responses and apoptosis [18]. In general, activation cascades are formed by a set of components (typically proteins) that become sequentially active in response to an external signal (see Fig. 1). The role of cascades is to relay, amplify, dampen or modulate signals in order to achieve a variety of cellular responses.

Activation cascades, particularly the MAPK cascade, have been the subject of numerous studies, experimental and theoretical [6, 7, 9, 12, 15, 16, 23, 26]. In this work, we study ODE models of linear cascades and obtain analytical solutions in terms of the lower incomplete gamma function for the case when inactivation rates are identical and study the case in which a single protein has a different inactivation rate to the rest. Finally, we discuss how these results may be used in parameter fitting and model reduction as an alternative to delay differential equations.

2. Linear cascades and their gamma function representation

Consider a cascade of length n subject to an external signal $\hat{R}(t)$. When receiving the input $\hat{R}(t)$, the first inactive component (x_1^*) is transformed

into its active state (x_1) which then activates the next inactive component (x_2^*). Sequential activation of x_i^* by x_{i-1} continues until the end of the cascade. The output of the cascade is the active form of the last protein, x_n. In the case of the MAPK cascade, the components are proteins and the activation corresponds to a post-translational modification, i.e., phosphorylation. However, the formalism below could also be used to describe other sequential biochemical processes with similar functional relationships, e.g. n-step DNA unwinding [17].

The mass-action kinetics model that describes the time evolution of the activation cascade is [12]:

$$\begin{aligned}
\frac{\mathrm{d}x_1}{\mathrm{d}t} &= \hat{R}(t)(T_1 - x_1) - \beta_1 x_1, \\
\frac{\mathrm{d}x_2}{\mathrm{d}t} &= \hat{\alpha}_2 x_1 (T_2 - x_2) - \beta_2 x_2, \\
&\vdots \\
\frac{\mathrm{d}x_n}{\mathrm{d}t} &= \hat{\alpha}_n x_{n-1} (T_n - x_n) - \beta_n x_n,
\end{aligned} \tag{1}$$

where $(T_i - x_i) = x_i^*$ is the inactive form of x_i when the total amount of each component is given by $T_i = x_i + x_i^*$. We assume resting initial conditions (i.e., $x_i(0) = 0$, for all i) and that T_i remains a constant (i.e., no protein production). As shown in Ref. [12], whenever $T_i \gg x_i$ we have $T_i - x_i \approx T_i$ (the so-called *weakly-activated* case) and we can re-write the system (1) as

$$\begin{aligned}
\frac{\mathrm{d}x_1}{\mathrm{d}t} &= R(t) - \beta_1 x_1, \\
\frac{\mathrm{d}x_2}{\mathrm{d}t} &= \alpha_2 x_1 - \beta_2 x_2, \\
&\vdots \\
\frac{\mathrm{d}x_n}{\mathrm{d}t} &= \alpha_n x_{n-1} - \beta_n x_n,
\end{aligned} \tag{2}$$

where $\alpha_i = \hat{\alpha}_i T_i$ and $R(t) = \hat{R}(t) T_1$.

The system of equations (2) is linear and can be written in vector form:

$$\dot{\mathbf{x}} = \mathbf{A}\mathbf{x} + R(t)\mathbf{e}_1, \tag{3}$$

where $\mathbf{x} = [x_1, \ldots, x_n]^T$, the $n \times n$ rate matrix $\mathbf{A}$ is:

$$\mathbf{A} = \begin{bmatrix} -\beta_1 & & & \\ \alpha_2 & -\beta_2 & & \\ & \ddots & \ddots & \\ & & \alpha_n & -\beta_n \end{bmatrix}, \tag{4}$$

and $\mathbf{e}_1 = [1, 0, \ldots, 0]^T$ is the first $n \times 1$ vector of the canonical basis. In general, we use $\mathbf{e}_i$ to denote the i-th canonical vector.

2.1. Constant stimulus

In an experimental setting, one often wants to study the response of a biological system to a constant stimulus (e.g., constant temperature, light or treatment):

$$R(t) = \alpha_1 \in \mathbb{R},\ t \geq 0.$$

Then the solution to equation (3) with initial condition $\mathbf{x}(0) = \mathbf{0}$ is:

$$\mathbf{x}(t) = \alpha_1 \mathbf{A}^{-1} \left[e^{t\mathbf{A}} - \mathbf{I}_n \right] \mathbf{e}_1, \tag{5}$$

where $\mathbf{I}_n$ is the $n \times n$ identity matrix, and $e^{t\mathbf{A}}$ is the matrix exponential.

Recently, it has been shown that, given a fixed gain, a linear cascade provides optimal amplification when all the inactivation rates are identical (i.e., $\beta_i = \beta$ for all i) and the cascade has a finite length [7].

Assume that our cascade is optimal with $\beta_i = \beta$, then the rate matrix becomes

$$\tilde{\mathbf{A}} = \begin{bmatrix} -\beta & & & \\ \alpha_2 & -\beta & & \\ & \ddots & \ddots & \\ & & \alpha_n & -\beta \end{bmatrix}, \tag{6}$$

and it can be shown (see Appendix A.1 and Ref. [17] for detailed calculations) that the solution for the output of the cascade is:

$$x_n(t) = \left(\frac{\alpha_{(n)}}{\beta} \right)^n \mathrm{P}(n, \beta t), \tag{7}$$

where $\mathrm{P}(n, \beta t)$ is the normalised lower incomplete gamma function and $\alpha_{(n)}$ is the geometric mean of the activation rates

$$\alpha_{(n)} = \left(\prod_{j=1}^{n} \alpha_j \right)^{1/n}. \tag{8}$$

2.2. Exponentially decreasing stimulus

When the first protein in the cascade is subject to an exponentially decaying stimulus (e.g., when the signal is a reactive molecule or it becomes metabolised, or the receptors become desensitised)

$$R(t) = \alpha_1 e^{-\lambda t},$$

then the solution to Eq. (3) with initial condition $\mathbf{x}(0) = \mathbf{0}$ is

$$\mathbf{x}(t) = \alpha_1 \left[e^{t\mathbf{A}} - e^{-\lambda t}\mathbf{I}_n\right] \mathbf{A}^{-1} \left[\mathbf{I}_n + \lambda \mathbf{A}^{-1}\right]^{-1} \mathbf{e}_1. \tag{9}$$

If we assume again that $\beta_i = \beta$ for all i (i.e., $\mathbf{A} = \tilde{\mathbf{A}}$), then the output of the system is given by:

$$x_n(t) = \begin{cases} \left(\frac{\alpha_{(n)}}{\beta-\lambda}\right)^n e^{-\lambda t}\, \mathrm{P}(n, (\beta-\lambda)t) & \text{if } \beta \neq \lambda \\ \\ \frac{1}{\Gamma(n+1)} \left(\alpha_{(n)} t\right)^n e^{-\beta t} & \text{if } \beta = \lambda, \end{cases} \tag{10}$$

where $\alpha_{(n)}$ is defined in (8) and $\Gamma(n+1)$ is the gamma function. As for the case of constant stimulus, the solution is also given in terms of the lower incomplete gamma function (see Appendix A.1 for calculations).

3. Perturbation of a single inactivation rate

We now examine how the output of a weakly-activated (linear) activation cascade is modified when a single protein in the cascade has a different inactivation rate. For instance, Ref. [7] considered a cascade with an auxiliary protein with different inactivation rate (i.e., a leaky integrator) at the end of the cascade. We study the effect of such a 'perturbation' and how the effect depends on the position of the component in the cascade.

Consider a cascade of n proteins with activation rates α_j and inactivation rates $\beta_j = \beta,\ \forall j \neq i$, and $\beta_i = \beta + \varepsilon$ for a given node i. In this case, the rate matrix of the system (3) is

$$\mathbf{A} = \tilde{\mathbf{A}} - \varepsilon\, \mathbf{e}_i \mathbf{e}_i^T \equiv \mathbf{H}_i, \tag{11}$$

where $\tilde{\mathbf{A}}$ is given in Eq. (6) and $\mathbf{e}_i$ is the i-th vector of the canonical basis in $\mathbb{R}^n$.

The Jordan decomposition of $\mathbf{H}_i$ is

$$\mathbf{H}_i = \mathbf{Q}_i \mathbf{J} \mathbf{Q}_i^{-1}, \tag{12}$$

where $\mathbf{J}$ is the Jordan normal form

$$\mathbf{J} = \begin{bmatrix} -(\beta+\varepsilon) & & & & & \\ & -\beta & 1 & & & \\ & & -\beta & \ddots & & \\ & & & \ddots & 1 & \\ & & & & -\beta \end{bmatrix}, \tag{13}$$

and $\mathbf{Q}_i$ is the matrix with generalised eigenvectors as columns.

An important property of this Jordan decomposition is that both $\mathbf{J}$ and the vector $\mathbf{Q}_i^{-1}\mathbf{e}_1$ are independent of the location of the perturbation i. As shown in Example 6, this follows from the following fact: consider $i < h$ (without loss of generality), then rows 1 to $i-1$ and h to n of $\mathbf{Q}_i$ and $\mathbf{Q}_h$ are identical, i.e., $\mathbf{Q}_i(1:i-1,:) = \mathbf{Q}_h(1:i-1,:)$ and $\mathbf{Q}_i(h:n,:) = \mathbf{Q}_h(h:n,:)$ in Matlab notation. (See proof in Appendix B.)

3.1. Constant stimulus

The constant stimulus solution (5) for the perturbed case ($\mathbf{A} = \mathbf{H_i}$) is

$$\mathbf{x}(t) = \alpha_1 \mathbf{H}_i^{-1} \left[e^{t\mathbf{H}_i} - \mathbf{I}_n \right] \mathbf{e}_1 = \alpha_1 \mathbf{Q}_i \mathbf{J}^{-1} \left[e^{t\mathbf{J}} - \mathbf{I}_n \right] \mathbf{Q}_i^{-1} \mathbf{e}_1, \tag{14}$$

which follows from (12). The properties of $\mathbf{J}$ and $\mathbf{Q}_i$ stated above imply that the vector $\mathbf{J}^{-1}\left[e^{t\mathbf{J}} - \mathbf{I}_n\right]\mathbf{Q}_i^{-1}\mathbf{e}_1$ is independent of the position of the perturbation, i. Hence the entries of $\mathbf{x}(t)$ are determined only by the matrix $\mathbf{Q}_i$. However, for two cascades with modified decay rates at i and h ($i < h$), we have $\mathbf{Q}_i(h:n,:) = \mathbf{Q}_h(h:n,:)$, meaning that the solution for the last $n-h+1$ proteins is the same in both cascades. (Similarly, the $i-1$ first components of the solution (14) are identical, but that is obvious.) Hence the position of the perturbation in the inactivation rate of a component does not affect the final output of the cascade.

Example 1. Consider two cascades of length $n = 6$ with constant stimulus and activation rates $\alpha_1 = \cdots = \alpha_6 = 3$ and degradation rate $\beta = 2$ for all

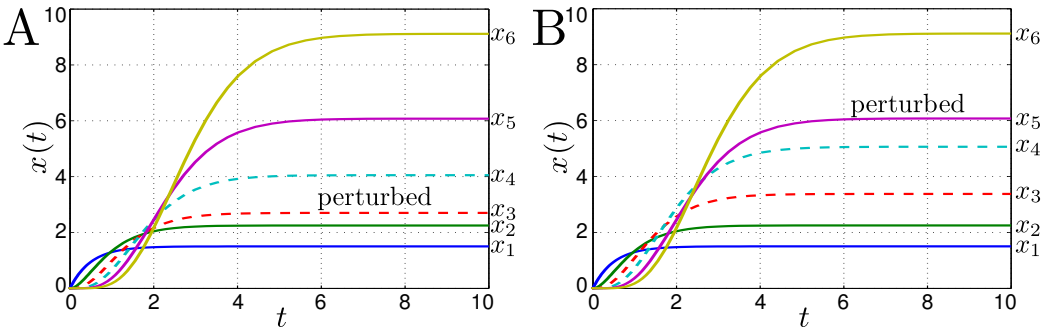

Figure 2: (Colour) Time course solutions of two ε-perturbed cascades from Example 1. **A**: Cascade with a perturbation in the degradation of the third protein. **B**: Cascade with a perturbation in the fifth protein. The activity of the proteins of both cascades in the same for nodes above and below the perturbations (continuous lines), but is different in the nodes between the perturbations (dashed lines).

proteins except for a perturbation $\varepsilon = 0.5$ on the third and fifth proteins of each cascade, respectively. The corresponding rate matrices are:

$$\mathbf{H}_3 = \begin{bmatrix} -2 & & & & & \\ 3 & -2 & & & & \\ & 3 & -2.5 & & & \\ & & 3 & -2 & & \\ & & & 3 & -2 & \\ & & & & 3 & -2 \end{bmatrix} \quad \mathbf{H}_5 = \begin{bmatrix} -2 & & & & & \\ 3 & -2 & & & & \\ & 3 & -2 & & & \\ & & 3 & -2 & & \\ & & & 3 & -2.5 & \\ & & & & 3 & -2 \end{bmatrix}.$$

The Jordan form for both cascades is:

$$\mathbf{J} = \begin{bmatrix} -2.5 & & & & & \\ & -2 & 1 & & & \\ & & -2 & 1 & & \\ & & & -2 & 1 & \\ & & & & -2 & 1 \\ & & & & & -2 \end{bmatrix}$$

and the corresponding generalised eigenvector matrices are:

$$\mathbf{Q}_3 = \begin{bmatrix} \mathbf{0} & \mathbf{0} & \mathbf{0} & \mathbf{0} & \mathbf{0} & \mathbf{1} \\ \mathbf{0} & \mathbf{0} & \mathbf{0} & \mathbf{0} & \mathbf{3} & \mathbf{0} \\ 36 & 0 & 0 & 0 & 18 & -36 \\ -216 & 0 & 0 & 54 & -108 & 216 \\ \mathbf{1296} & \mathbf{0} & \mathbf{162} & \mathbf{-324} & \mathbf{648} & \mathbf{-1296} \\ \mathbf{-7776} & \mathbf{486} & \mathbf{-972} & \mathbf{1944} & \mathbf{-3888} & \mathbf{7776} \end{bmatrix}, \tag{15}$$

$$\mathbf{Q}_5 = \begin{bmatrix} \mathbf{0} & \mathbf{0} & \mathbf{0} & \mathbf{0} & \mathbf{0} & \mathbf{1} \\ \mathbf{0} & \mathbf{0} & \mathbf{0} & \mathbf{0} & \mathbf{3} & \mathbf{0} \\ 0 & 0 & 0 & 9 & 0 & 0 \\ 0 & 0 & 27 & 0 & 0 & 0 \\ \mathbf{1296} & \mathbf{0} & \mathbf{162} & \mathbf{-324} & \mathbf{648} & \mathbf{-1296} \\ \mathbf{-7776} & \mathbf{486} & \mathbf{-972} & \mathbf{1944} & \mathbf{-3888} & \mathbf{7776} \end{bmatrix}. \tag{16}$$

As explained above, rows 1-2 and 5-6 of $\mathbf{Q}_3$ and $\mathbf{Q}_5$ (in bold) are the same. In addition,

$$\mathbf{Q}_3^{-1}\mathbf{e}_1 = \mathbf{Q}_5^{-1}\mathbf{e}_1 = \begin{bmatrix} 1 \\ 0 \\ 0 \\ 0 \\ 0 \\ 1 \end{bmatrix}$$

Since the rows of of $\mathbf{Q}_3$ and $\mathbf{Q}_5$ are the same below the second perturbation, then the values of $x_5(t)$ and $x_6(t)$ are equal in both cascades. Figure 2 shows the time course of the proteins in both cascades: $x_1(t)$, $x_2(t)$, $x_5(t)$, and $x_6(t)$ (solid lines) are the same in both cascades, while $x_3(t)$ and $x_4(t)$, the proteins "sandwiched" between the perturbations (dashed lines), are not. We discuss an application of this result in Section 4.2.

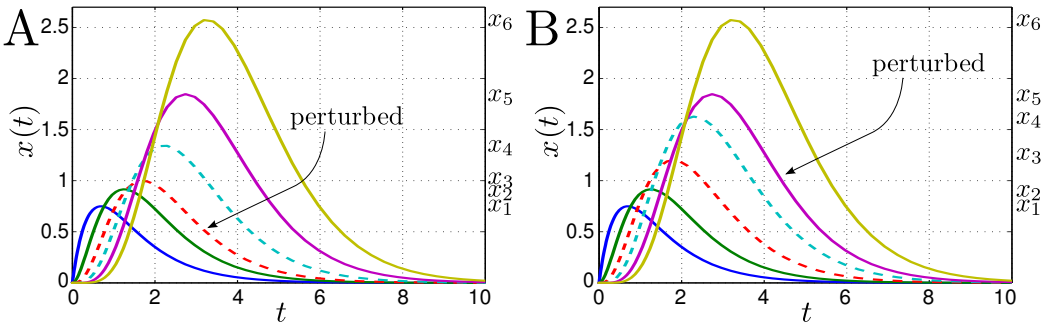

Figure 3: (Colour) Time course solutions of two ε-perturbed cascades with decaying stimulus from Example 2. **A**: Cascade with a perturbation in the third protein. **B**: Cascade with a perturbation in the fifth protein. On the right of each plot, the label of each protein is placed at the level where its solution peaks. The activity of the proteins is the same for nodes above and below the perturbations (continuous lines), but different in the nodes between the perturbations (dashed lines).

3.2. Exponentially decreasing stimulus

Just as in the previous section, the solution (9) for the exponential stimulus in the perturbed case ($\mathbf{A} = \mathbf{H_i}$) can be rewritten as:

$$\mathbf{x}(t) = \alpha_1 \mathbf{Q}_i \left[e^{t\mathbf{J}} - e^{-\lambda t} \mathbf{I}_n \right] \mathbf{J}^{-1} \left[\mathbf{I}_n + \lambda \mathbf{J}^{-1} \right]^{-1} \mathbf{Q}_i^{-1} \mathbf{e}_1, \tag{17}$$

and, again, the same argument follows to conclude that the last $n - h + 1$ components of the solution (17) are the same for two cascades modified at positions i and h ($h > i$).

Example 2. Consider the same cascades as in Example 1 with stimulus $R(t) = \alpha_1 e^{-\lambda t}$ with $\lambda = 1$. Figure 3 shows the time behaviour of the proteins in the two cascades. As in the previous example, the proteins above and below the perturbations are unchanged.

4. Applications

4.1. Model simplification and parameter fitting

The expressions for the output of the cascade $x_n(t)$ in terms of incomplete gamma functions can be useful to fit activation data to a reduced number of parameters. Rather than fitting the observed output of the cascade to $n + 2$ parameters for an entire module with n components, the approximate expression with the lower incomplete gamma function contains at most four

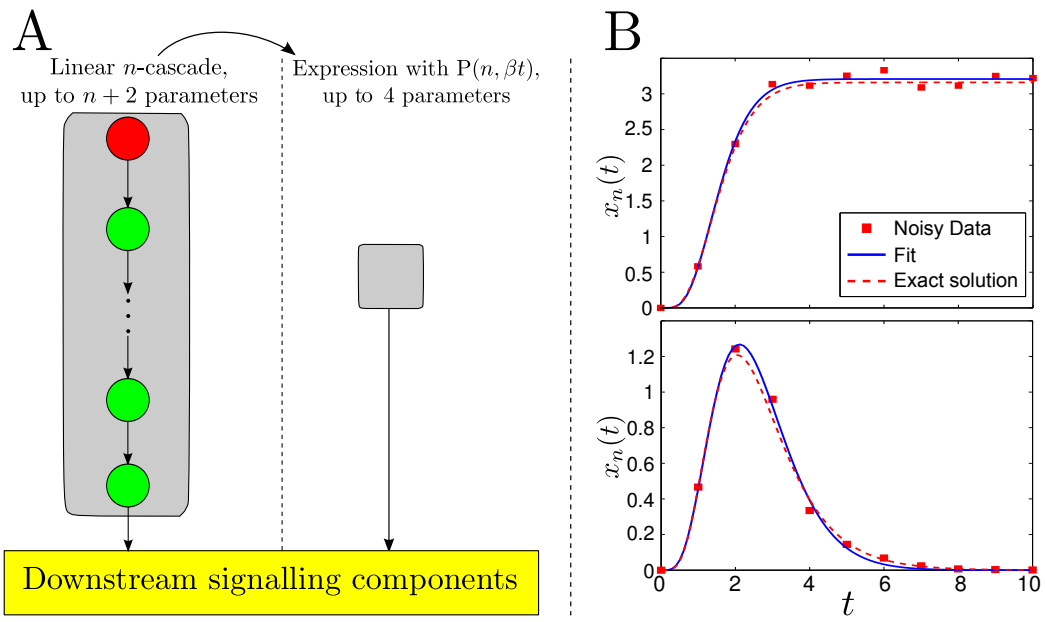

Figure 4: (Colour) **A**: Schematic of a signal transduction model with a cascade. Given a linear cascade of arbitrary length, the red node node at the top is the stimulus, and green nodes are the components of the cascade. The last node of the cascade transmits the signal to downstream components of the pathway. The model of the cascade has up to $n+2$ parameters: $\alpha_1, \ldots, \alpha_n$, β, and if the stimulus decays, λ. Then the cascade is condensed into an expression with an incomplete gamma function that sends the exact same signal as the cascade in the left panel directly to the rest of the network. The new expression has parameters $\alpha_{(n)}$, β, n, and if the stimulus decays, λ. **B**: Examples of the time-course of two cascades with constant (top) and exponentially decaying stimulus (bottom). The dashed lines indicate the solutions to the corresponding systems of ODEs, squares are noisy data generated from the models, and bold lines are fits to the data using the incomplete gamma function expressions (see Example 3).

parameters: $\alpha_{(n)}$, β, n (and in the case of exponential decay, λ). In this approach, (shown graphically in Fig. 4A) the length of the cascade n is turned into a fitting parameter, similarly to what is done with Hill coefficients. Indeed, the fitted value does not need to be an integer because the lower incomplete gamma function $\mathrm{P}(n,t)$ is defined for any positive real number in its first argument [1].

Example 3. Consider two cascades of length $n = 5$ with parameters $\alpha_1 = 3$, $\alpha_i = 4$ for $i = 2, \ldots, 5$ (so $\alpha_{(n)} = 3.776$), and $\beta = 3$. One cascade is subject to a constant stimulus $R(t) = \alpha_1$ and the other to an exponentially decaying input $R(t) = \alpha_1 e^{-\lambda t}$ with $\lambda = 1$.

After solving numerically the ODE models of the linear cascade (3) for both inputs (dashed lines in Fig. 4B), we sample the output $x_5(t)$ at times $t = \{0, 1, \ldots, 10\}$ and we add random noise from a distribution $\mathcal{N}(0, 0.05^2)$ to generate our 'observed data' (squares in Fig. 4B).

We fit the gamma function expressions (7) and (10) to the 'data' using the parameter fitting method introduced in Ref. [3] (see Appendix D). The bold lines in Fig. 4B show the fits to both cascade output data. The fits to the noisy data are good and the estimated values are close to the 'true' ones: in the case of the constant stimulus cascade, the fitted values are $\alpha_{(n)} \approx 4.068$, $\beta \approx 3.281$, and $n \approx 5.418$; in the case of the exponentially decaying stimulus, the estimated values are $\alpha_{(n)} \approx 3.317$, $\beta \approx 2.177$, $n \approx 4.6$, and $\lambda \approx 2.177$.

4.2. Cascade equation reordering

The results presented in Sec. 2 and 3 allow us to reshuffle equations of cascade models where perturbations are known to occur. In particular, all proteins with the same inactivation rates can be grouped together upstream in the cascade so that they can be replaced with the incomplete gamma function expression, while the perturbed proteins are placed downstream and take the gamma function as an input.

This process of reordering the cascade, which is schematically represented in Fig. 5A, can be used to reduce the ODE model for the cascade without altering the dynamics or the timescales. Suppose we have an ε-perturbed cascade of $n+1$ proteins that we have reordered so that the first n proteins have inactivation rate β and the $(n+1)$-th protein has rate $\beta + \varepsilon$.

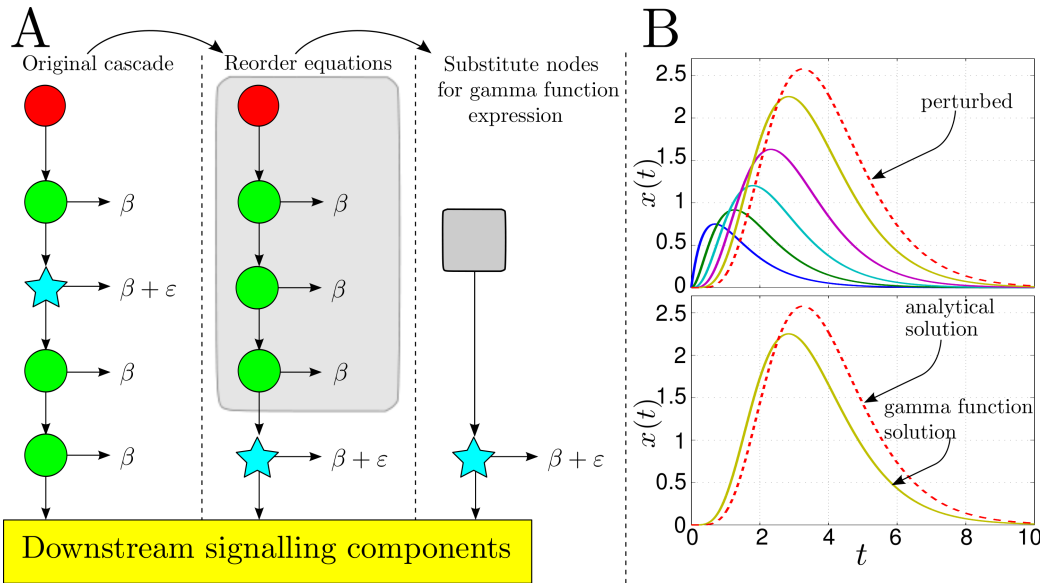

Figure 5: (Colour) Example of cascade reordering and substitution. **A**: A linear ε-perturbed cascade model of length 4, the input (red node) can either be constant or decaying. Green circle nodes are proteins whose inactivation rates are all β, the blue star node has inactivation rate $\beta + \varepsilon$. Downstream of the cascade lie other components of the signalling pathway. Reordering of the equations: the protein with the perturbed inactivation has been moved the bottom of the cascade. Both this cascade and the one on the left have the same output. The first three equations in the reordered cascade are substituted for an incomplete gamma function. **B**: Numerical example of cascade reordering. Top: the equation of the perturbed protein is placed at the bottom of the cascade (the time-course of the untouched cascade is shown in Fig. 3A). Bottom: the solution to the module of unperturbed proteins is given by equation (10); the solution of the perturbed protein at the bottom of the cascade is given by equation (21) (see Example 4).

4.2.1. Constant input

Consider first a constant input $R(t) = \alpha_1$. Using (7), we write the dynamics of the output of the cascade as

$$\frac{\mathrm{d}x_{n+1}}{\mathrm{d}t} = \alpha_{n+1}\left(\frac{\alpha_{(n)}}{\beta}\right)^n \mathrm{P}(n, \beta t) - (\beta + \varepsilon)x_{n+1}. \tag{18}$$

This equation can be solved analytically (see Appendix C.1):

$$x_{n+1}(t) = \frac{\alpha_{n+1}}{\beta + \varepsilon}\left(\frac{\alpha_{(n)}}{\beta}\right)^n \left(1 - e^{-\beta t}\left[\left(\frac{-\beta}{\varepsilon}\right)^n e^{-\varepsilon t} + \sum_{k=0}^{n-1} \frac{(\varepsilon^{n-k} - (-\beta)^{n-k})(\beta t)^k}{\varepsilon^{n-k} k!}\right]\right), \tag{19}$$

where we have taken the initial condition $x_{n+1}(0) = 0$.

4.2.2. Exponentially decaying input

Consider an exponentially decaying input $R(t) = \alpha_1 e^{-\lambda t}$. First assume $\beta \neq \lambda$, and use (10) to write the ODE for the $(n+1)$-th protein:

$$\frac{\mathrm{d}x_{n+1}}{\mathrm{d}t} = \alpha_{n+1}\left(\frac{\alpha_{(n)}}{\beta-\lambda}\right)^n e^{-\lambda t}\,\mathrm{P}(n,(\beta-\lambda)t) - (\beta+\varepsilon)x_{n+1}. \tag{20}$$

When the initial condition is $x_{n+1}(0) = 0$, the analytical solution for this equation is (see Appendix C.2):

$$x_{n+1}(t) = \frac{\alpha_{n+1}}{\beta-\lambda+\varepsilon}\left(\frac{\alpha_{(n)}}{\beta-\lambda}\right)^n \left[e^{-\lambda t} + \frac{e^{-(\beta+\varepsilon)t}}{\varepsilon^n} - \right.$$
$$\left. - e^{-\beta t}\sum_{k=0}^{n-1}\frac{\left(\varepsilon^{n-k} - (\lambda-\beta)^{n-k}\right)(\beta-\lambda)^k t^k}{\varepsilon^{n-k}k!}\right]. \tag{21}$$

When $\beta = \lambda$ we have:

$$\frac{\mathrm{d}x_{n+1}}{\mathrm{d}t} = \alpha_{n+1}\frac{\left(\alpha_{(n)}t\right)^n}{\Gamma(n+1)}\,e^{-\beta t} - (\beta+\varepsilon)x_{n+1}, \tag{22}$$

and the solution is

$$x_{n+1}(t) = \left(\frac{\alpha_{(n+1)}}{\varepsilon}\right)^{n+1} e^{-\beta t}\left[\varepsilon^n\sum_{k=0}^{n}\frac{(-1)^k t^{n-k}}{\varepsilon^k(n-k)!} + (-1)^{n+1}e^{-\varepsilon t}\right]. \tag{23}$$

Example 4. Consider the $n = 6$ cascade from Example 2, where the degradation rate of the third protein is ε-perturbed (time-course shown in Fig. 2A). The equations of the system can be reordered without affecting its final output so that the equation of the perturbed protein is at the bottom of the cascade (Fig. 5B, top). The output of the first 5 equations in the reordered cascade is then given by the incomplete gamma function expression (10) and the analytical solution of the perturbed protein (which is now the output of the cascade) is given by Eq. (21) (Fig. 5B, bottom).

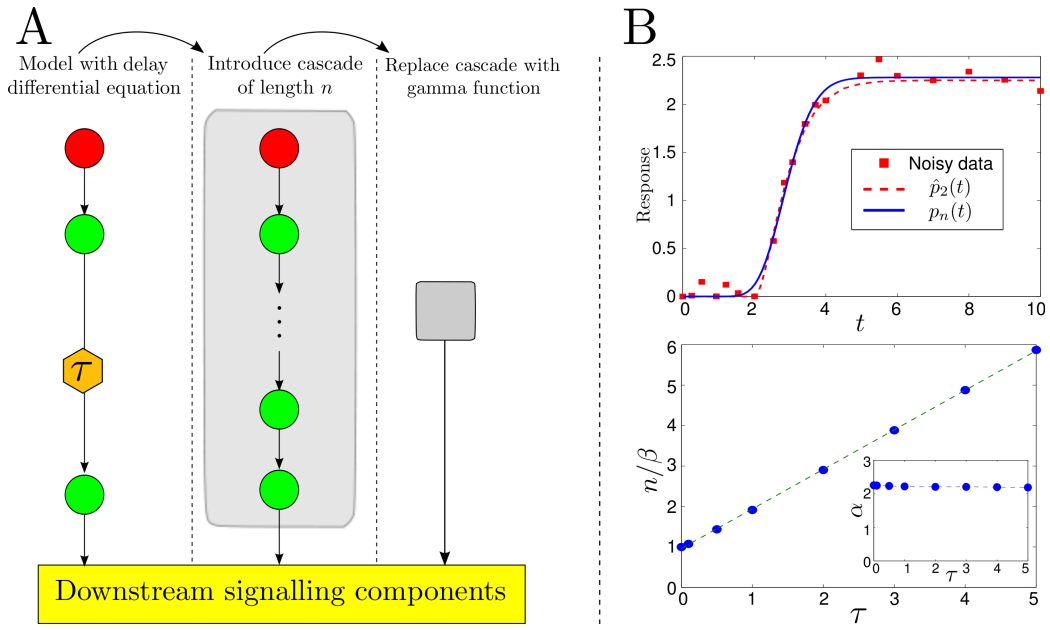

Figure 6: (Colour) **A**: Example of the use of linear activation cascades to replace delay differential equations. A signal node (red node) activates a node in a signalling pathway. The bottom node responds with a delay τ. The delay in the equation is removed and substituted with a linear cascade of length n. The entire cascade is replaced by a lower incomplete gamma function. **B**: Top: The dashed line is the solution to the DDE (24) from Example 5, the squares are points taken from the solution with added random noise. The continuous line is the approximation using a lower incomplete gamma function. Bottom: the relationship between the ratio n/β and τ is linear (dashed-line) with slope 0.977 and intercept 0.962. Inset: α almost does not vary with τ (see text).

4.3. Delay differential equation models for activation cascades

Experimental observations in signalling cascades are typically concerned with the effect of the cascade on the output characterised in terms of the amplification, distortion and delay introduced in the output downstream. Within the framework of ODE models, the interactions between the variables occur instantaneously. Hence, if the response to a stimulus occurs with delay, one must incorporate further intermediate variables that were not considered in the original ODE model, corresponding to unmeasured, hidden processes that take time to complete [21]. This process can lead to large models with many unobservable variables and large numbers of parameters or to the introduction of abstract variables to model unknown processes that may contribute to the observed delays [2, 13]. Alternatively, modellers

often use delay differential equations (DDEs) to account for the wait between an event and its effect parsimoniously [5, 8, 19]. In a DDE, the activity of a variable depends on the state of the system in the past:

$$\frac{\mathrm{d}\mathbf{x}}{\mathrm{d}t} = \mathbf{f}(\mathbf{x}(t-\tau)),$$

where the parameter $\tau \geq 0$ is the delay. Linear systems of delay differential equations can be solved analytically using infinite series involving the Lambert function [4, 25], but such solutions are often impractical to use. Our results indicate that simple delays can be modelled with linear activation cascades leading to concise ODE descriptions in terms of the lower incomplete gamma function and without relying on DDEs, as shown in Figure 6A.

Example 5. Consider a system with a delay, which we model with the following linear DDE:

$$\begin{aligned} \frac{\mathrm{d}\hat{p}_1}{\mathrm{d}t} &= \hat{\alpha} - \hat{\beta}\,\hat{p}_1, \\ \frac{\mathrm{d}\hat{p}_2}{\mathrm{d}t} &= \hat{\alpha}\,\hat{p}_1(t-\tau) - \hat{\beta}\,\hat{p}_2. \end{aligned} \tag{24}$$

Figure 6B (top plot) shows the simulated time course of $\hat{p}_2(t)$ (red dashed line) when $\hat{\alpha} = 2$, $\hat{\beta} = 3$, and $\tau = 2$ with initial conditions $\hat{p}_1(0) = \hat{p}_2(0) = 0$. To generate our 'observed data,' we sample $\hat{p}_2$ at various time points and add observational random noise from a distribution $\mathcal{N}(0, 0.05^2)$.

We can fit this noisy data to a linear cascade of length n under constant input with parameters $\alpha_{(n)}$ and β:

$$p_n(t) = \left(\frac{\alpha_{(n)}}{\beta}\right)^n \mathrm{P}(n, \beta t) \approx \hat{p}_2(t), \tag{25}$$

and estimate the corresponding parameters. The solid line in the top plot of Fig. 6B shows the best fit of the data to a linear cascade, as obtained with a parameter fitting algorithm (see Appendix D). The estimated parameter values are $\alpha_{(n)} \approx 2.27$, $\beta \approx 7.53$, and $n \approx 22.1072$.

We also explore the connection between the parameters of the DDE and the best fitted (linear) activation cascade model, in particular as a function of the delay τ. We simulate the DDE (24) with parameters $\hat{\alpha} = 2$ and $\hat{\beta} = 3$) for different values of the delay $\tau \in [0, 5]$ and collect data from these models

as above, but without adding random noise. The dependence of the fitted parameters and τ is shown in Fig. 6B (bottom plot): α remains relatively constant while the ratio n/β grows almost linearly with τ $n/\beta = 0.962 + 0.977\tau$. In fact, β increases linearly (slope ≈ 4.11) and n grows almost quadratically with τ (exponent ≈ 1.88). When the delay τ in the 'data' is increased, the length of the fitted cascade (n) increases while the time scale of the gamma function ($1/\beta$) decreases in consortium. If one attempts to fit the data allowing only the length n as a fitting parameter, the fit is not successful, thus underscoring the importance of the time scale β in the approximation. Indeed, the original time delay τ in the DDE is approximated in the linear cascade by $(n/\beta - 1)$, i.e., the accumulated time needed to traverse n sequential steps with duration $1/\beta$.

5. Conclusions

We have examined the classic model of activation cascades in the weakly activated limit [12]. Following recent results [7], we have considered the important case where all inactivation rates of the components of the cascade are identical, which has been shown to provide optimal amplification. Our results show that the output of these cascades can be represented exactly by lower incomplete gamma functions. We also show that when one protein in the cascade has a different inactivation rate than the rest, its position in the cascade does not affect the final output. We have used these results to reduce the number of equations and parameters in ODE models without affecting the dynamics or the timescales of the system. We also show that in some cases incomplete gamma functions can be used to approximate delay differential equations. Beyond its application to enzymatic activation cascades, similar mathematical models of cascades could be helpful for the parametrisation and modelling of multi-step transcriptional processes, an area of active research in Systems and Synthetic Biology [14, 17, 22, 24].

Acknowledgments

The authors thank S. Moon, J. Stark, M. Stumpf, R. Tanaka, B. Wang and S. Yaliraki for valuable discussions and comments. MBD is supported by a BBSRC-Microsoft Research Dorothy Hodgkin Postgraduate Award and though partial funding from the U.S. Office of Naval Research. MB acknowledges support from BBSRC LoLa grant BB/G020434/1 and BBSRC SABR grant BB/F005210/2.

Appendix A. Calculation of the output of the linear cascade, $x_n(t)$

Appendix A.1. The incomplete gamma function: Definitions and notation [1]

The gamma function is defined as:

$$\Gamma(a) = \int_0^\infty e^{-s} s^{a-1} \mathrm{d}s, \qquad \mathrm{Re}(a) > 0. \tag{A.1}$$

One property of the gamma function is $\Gamma(n) = (n-1)!$, $n \in \mathbb{N}$.

The *lower incomplete* gamma function is given by:

$$\gamma(a,t) = \int_0^t e^{-s} s^{a-1} \mathrm{d}s, \qquad \mathrm{Re}(a) > 0 \tag{A.2}$$

A different way of writing $\gamma(a,t)$ when $a = n \in \mathbb{N}$ is [20]:

$$\gamma(n,t) = (n-1)! \left(1 - e^{-t} \sum_{k=0}^{n-1} \frac{t^k}{k!}\right). \tag{A.3}$$

The *normalised* lower incomplete gamma function, which we use in our calculations, is defined as:

$$\mathrm{P}(a,t) = \frac{\gamma(a,t)}{\Gamma(a)}. \tag{A.4}$$

Appendix A.2. Constant stimulus: derivation of Eq. (7)

The solution of the ODE system (3) for $\mathbf{x}(0) = 0$ is given in Eq. (5):

$$\mathbf{x}(t) = \alpha_1 \mathbf{A}^{-1} \left[e^{t\mathbf{A}} - \mathbf{I}_n\right] \mathbf{e}_1. \tag{A.5}$$

It can be shown by mathematical induction that the n-th component of the solution is:

$$x_n(t) = \left(\frac{\alpha_{(n)}}{\beta}\right)^n \left(1 - e^{-\beta t} \sum_{k=0}^{n-1} \frac{(\beta t)^k}{k!}\right). \tag{A.6}$$

A similar result is obtained in Ref. [17] from the analysis of linear models of DNA unwinding.

Using (A.3) and the properties of the gamma function equation (A.6) becomes:

$$x_n(t) = \left(\frac{\alpha_{(n)}}{\beta}\right)^n \frac{\gamma(n,\beta t)}{\Gamma(n)} = \left(\frac{\alpha_{(n)}}{\beta}\right)^n \mathrm{P}(n,\beta t). \tag{A.7}$$

Appendix A.3. Exponentially decaying stimulus: derivation of Eq. (10)

The solution of the ODE system (3) for $\mathbf{x}(0) = 0$ is given in (9):

$$\mathbf{x}(t) = \alpha_1 \left[e^{t\mathbf{A}} - e^{-\lambda t}\mathbf{I}_n\right] \mathbf{A}^{-1} \left[\mathbf{I}_n + \lambda \mathbf{A}^{-1}\right]^{-1} \mathbf{e}_1. \tag{A.8}$$

When $\beta \neq \lambda$, we can use mathematical induction to show that

$$x_n(t) = \left(\frac{\alpha_{(n)}}{\beta - \lambda}\right)^n \left(e^{-\lambda t} - e^{-\beta t} \sum_{k=0}^{n-1} \frac{t^k (\beta - \lambda)^k}{k!}\right) \tag{A.9}$$

$$= \left(\frac{\alpha_{(n)}}{\beta - \lambda}\right)^n e^{-\lambda t} \frac{\gamma(n, (\beta - \lambda)t)}{\Gamma(n)} = \left(\frac{\alpha_{(n)}}{\beta - \lambda}\right)^n e^{-\lambda t} \mathrm{P}(n, (\beta - \lambda)t). \tag{A.10}$$

When $\beta = \lambda$, we solve sequentially the ODEs (3) and use mathematical induction to get

$$x_n(t) = \frac{\left(\alpha_{(n)} t\right)^n e^{-\beta t}}{\Gamma(n+1)}. \tag{A.11}$$

Appendix B. Properties of the ε-perturbed matrix of rates, $\mathbf{H}_i$

The matrix $\mathbf{H}_i$, which corresponds to a linear cascade with a perturbation ε at position i, is defined in Eq. (11) and has a Jordan decomposition given in Eq. (12):

$$\mathbf{H}_i = \mathbf{Q}_i \mathbf{J} \mathbf{Q}_i^{-1}. \tag{B.1}$$

As can be seen from the lower-triangular structure of $\mathbf{H}_i$, its Jordan form is the direct sum of two Jordan blocks associated with $-(\beta + \varepsilon)$, with multiplicity 1, and $-\beta$, with multiplicity $n - 1$:

$$\mathbf{J} = \mathbf{J}_{-(\beta+\varepsilon)} \oplus \mathbf{J}_{-\beta}, \tag{B.2}$$

where

$$\mathbf{J}_{-(\beta+\varepsilon)} = \left[-(\beta + \varepsilon)\right]_{1\times 1}, \qquad \mathbf{J}_{-\beta} = \begin{bmatrix} -\beta & 1 & & \\ & -\beta & \ddots & \\ & & \ddots & 1 \\ & & & -\beta \end{bmatrix}_{(n-1)\times(n-1)}. \tag{B.3}$$

The matrix $\mathbf{Q}_i$ contains the generalised eigenvectors $\{\mathbf{q}_\ell^i\}_{\ell=1}^n$ as columns [10]:

$$\mathbf{Q}_i = \left[\mathbf{q}_1^i | \mathbf{q}_2^i | \ldots | \mathbf{q}_n^i\right].$$

Proposition 1. The following properties hold for $\mathbf{Q}_i$ and $\mathbf{J}$:

I. $\mathbf{J}$ is independent of i.

II. $\mathbf{q}_1^i$, the eigenvector of $\mathbf{H}_i$ associated with $-(\beta+\varepsilon)$, is given by:

$$\mathbf{q}_1^i(j) = \begin{cases} 0 & \text{if } j < i, \\ \alpha_{(j)}^j \left(\frac{-1}{\varepsilon}\right)^{j-1} & \text{if } j \geq i. \end{cases} \tag{B.4}$$

III. $\{\mathbf{q}_{n-k+1}^i\}_{k=1}^{n-1}$, the $(n-1)$ generalised eigenvectors of $\mathbf{H}_i$ associated with $-\beta$, are given by:

- If $i \leq k$

$$\mathbf{q}_{n-k+1}^i(j) = \begin{cases} 0 & j \in \{1 \dots k\}, \\ -\alpha_{(j)}^j \left(\frac{-1}{\varepsilon}\right)^{j-k} & j \in \{k+1 \dots n\}. \end{cases} \tag{B.5}$$

- If $i > k$

$$\mathbf{q}_{n-k+1}^i(j) = \begin{cases} 0 & j \in \{1 \dots i-1\} \backslash k, \\ \alpha_{(k)}^k & j = k, \\ -\alpha_{(j)}^j \left(\frac{-1}{\varepsilon}\right)^{j-k} & j \in \{i \dots n\}. \end{cases} \tag{B.6}$$

IV. The inverse of the transition matrix $\mathbf{Q}_i^{-1}$ has the following structure:

- The first row is

$$\mathbf{Q}_i^{-1}(1,j) = \begin{cases} \frac{(-\varepsilon)^{j-1}}{\alpha_{(j)}^j} & \text{if } j \leq i, \\ 0 & \text{if } j > i. \end{cases} \tag{B.7}$$

- Rows $k \in \{2, \dots, n\}$ are

$$\mathbf{Q}_i^{-1}(k,j) = \begin{cases} 0 & \text{if } j \leq n-k, \\ \frac{1}{\alpha_{(j)}^j} & \text{if } j = n-k+1, \\ \frac{\varepsilon}{\alpha_{(j)}^j} & \text{if } j = n-k+2 \text{ and } n-i+1 \geq k, \\ 0 & \text{otherwise.} \end{cases} \tag{B.8}$$

V. For all i:

$$\mathbf{Q}_i^{-1}\mathbf{e}_1 = \mathbf{e}_1 + \mathbf{e}_n = \begin{bmatrix} 1 \\ 0 \\ \vdots \\ 1 \end{bmatrix}. \tag{B.9}$$

Proof. I. All the matrices $\mathbf{H}_i$ have the same eigenvalues with the same multiplicity so the Jordan form $\mathbf{J}$ is identical for all i.

II. Let $\mathbf{v}_1^i = \mathbf{H}_i\mathbf{q}_1^i$, if $i = 1$ it is straightforward to see that $\mathbf{v}_1^1(1) = -(\beta+\varepsilon)$ and when $j > i$

$$\mathbf{v}_1^1(j) = \alpha_j\alpha_{(j-1)}^{j-1}\left(\frac{-1}{\varepsilon}\right)^{j-2} - \beta\alpha_{(j)}^{j}\left(\frac{-1}{\varepsilon}\right)^{j-1} = -(\beta+\varepsilon)\alpha_{(j)}^{j}\left(\frac{-1}{\varepsilon}\right)^{j-1}, \tag{B.10}$$

so $\mathbf{v}_1^1 = -(\beta+\varepsilon)\mathbf{q}_1^1$.
When $i > 1$ then $\mathbf{v}_1^i(j) = 0$ for $j = 1 \dots i-1$. If $j = i$, then

$$\mathbf{v}_1^j(i) = -(\beta+\varepsilon)\alpha_{(i)}^{i}\left(\frac{-1}{\varepsilon}\right)^{i-1},$$

and if $j > i$ then the same situation as in equation (B.10) applies, so again we have $\mathbf{v}_1^i = -(\beta+\varepsilon)\mathbf{q}_1^i$.

III. Define $\mathbf{B}_i = (\mathbf{H}_i + \beta\mathbf{I}_n)$, we can see from the definition of $\mathbf{q}_2^i$ in equations (B.5) and (B.6) that $\mathbf{B}_i\mathbf{q}_2^i = \mathbf{0}$, i.e., $\mathbf{q}_2^i$ is the eigenvector of $\mathbf{H}_i$ associated to $-\beta$. The rest of the generalised eigenvectors $\mathbf{q}_3^i \dots \mathbf{q}_n^i$ associated with $-\beta$ can be multiplied by $\mathbf{B}_i$ to show that

$$\mathbf{B}_i\mathbf{q}_h^i = \mathbf{q}_{h-1}^i, \qquad h = 3 \dots n. \tag{B.11}$$

It follows that $\mathbf{B}_i^{h-1}\mathbf{q}_h^i = \mathbf{0}$, so $\mathbf{Q}_i$ as defined in equations (B.4), (B.5), and (B.6) is the transition matrix of generalised eigenvectors of $\mathbf{H}_i$.

IV. We can verify that $\mathbf{Q}_i^{-1}$ defined in equations in equations (B.7) and (B.8) is the inverse of the transition matrix $\mathbf{Q}_i$ by multiplying them to obtain $\mathbf{Q}_i^{-1}\mathbf{Q}_i = \mathbf{I}_n$.

V. This property follows directly from the structure of $\mathbf{Q}_i^{-1}$.

□

Example 6. Consider a cascade of length $n = 6$. The structures of the transition matrix and its inverse for $i = 1, \ldots, 6$ are

$$\mathbf{Q}_1 = \begin{bmatrix} \alpha_{(1)} & 0 & 0 & 0 & 0 & 0 \\ -\frac{\alpha^2_{(2)}}{\varepsilon} & 0 & 0 & 0 & 0 & \frac{\alpha^2_{(2)}}{\varepsilon} \\ \frac{\alpha^3_{(3)}}{\varepsilon^2} & 0 & 0 & 0 & \frac{\alpha^3_{(3)}}{\varepsilon} & -\frac{\alpha^3_{(3)}}{\varepsilon^2} \\ -\frac{\alpha^4_{(4)}}{\varepsilon^3} & 0 & 0 & \frac{\alpha^4_{(4)}}{\varepsilon} & -\frac{\alpha^4_{(4)}}{\varepsilon^2} & \frac{\alpha^4_{(4)}}{\varepsilon^3} \\ \frac{\alpha^5_{(5)}}{\varepsilon^4} & 0 & \frac{\alpha^5_{(5)}}{\varepsilon} & -\frac{\alpha^5_{(5)}}{\varepsilon^2} & \frac{\alpha^5_{(5)}}{\varepsilon^3} & -\frac{\alpha^5_{(5)}}{\varepsilon^4} \\ -\frac{\alpha^6_{(6)}}{\varepsilon^5} & \frac{\alpha^6_{(6)}}{\varepsilon} & -\frac{\alpha^6_{(6)}}{\varepsilon^2} & \frac{\alpha^6_{(6)}}{\varepsilon^3} & -\frac{\alpha^6_{(6)}}{\varepsilon^4} & \frac{\alpha^6_{(6)}}{\varepsilon^5} \end{bmatrix}, \quad \mathbf{Q}_1^{-1} = \begin{bmatrix} \frac{1}{\alpha_{(1)}} & 0 & 0 & 0 & 0 & 0 \\ 0 & 0 & 0 & 0 & \frac{1}{\alpha^5_{(5)}} & \frac{\varepsilon}{\alpha^6_{(6)}} \\ 0 & 0 & 0 & \frac{1}{\alpha^4_{(4)}} & \frac{\varepsilon}{\alpha^5_{(5)}} & 0 \\ 0 & 0 & \frac{1}{\alpha^3_{(3)}} & \frac{\varepsilon}{\alpha^4_{(4)}} & 0 & 0 \\ 0 & \frac{1}{\alpha^2_{(2)}} & \frac{\varepsilon}{\alpha^3_{(3)}} & 0 & 0 & 0 \\ \frac{1}{\alpha_{(1)}} & \frac{\varepsilon}{\alpha^2_{(2)}} & 0 & 0 & 0 & 0 \end{bmatrix}, \tag{B.12}$$

$$\mathbf{Q}_2 = \begin{bmatrix} 0 & 0 & 0 & 0 & 0 & \alpha_{(1)} \\ -\frac{\alpha^2_{(2)}}{\varepsilon} & 0 & 0 & 0 & 0 & \frac{\alpha^2_{(2)}}{\varepsilon} \\ \frac{\alpha^3_{(3)}}{\varepsilon^2} & 0 & 0 & 0 & \frac{\alpha^3_{(3)}}{\varepsilon} & -\frac{\alpha^3_{(3)}}{\varepsilon^2} \\ -\frac{\alpha^4_{(4)}}{\varepsilon^3} & 0 & 0 & \frac{\alpha^4_{(4)}}{\varepsilon} & -\frac{\alpha^4_{(4)}}{\varepsilon^2} & \frac{\alpha^4_{(4)}}{\varepsilon^3} \\ \frac{\alpha^5_{(5)}}{\varepsilon^4} & 0 & \frac{\alpha^5_{(5)}}{\varepsilon} & -\frac{\alpha^5_{(5)}}{\varepsilon^2} & \frac{\alpha^5_{(5)}}{\varepsilon^3} & -\frac{\alpha^5_{(5)}}{\varepsilon^4} \\ -\frac{\alpha^6_{(6)}}{\varepsilon^5} & \frac{\alpha^6_{(6)}}{\varepsilon} & -\frac{\alpha^6_{(6)}}{\varepsilon^2} & \frac{\alpha^6_{(6)}}{\varepsilon^3} & -\frac{\alpha^6_{(6)}}{\varepsilon^4} & \frac{\alpha^6_{(6)}}{\varepsilon^5} \end{bmatrix}, \quad \mathbf{Q}_2^{-1} = \begin{bmatrix} \frac{1}{\alpha_{(1)}} & -\frac{\varepsilon}{\alpha^2_{(2)}} & 0 & 0 & 0 & 0 \\ 0 & 0 & 0 & 0 & \frac{1}{\alpha^5_{(5)}} & \frac{\varepsilon}{\alpha^6_{(6)}} \\ 0 & 0 & 0 & \frac{1}{\alpha^4_{(4)}} & \frac{\varepsilon}{\alpha^5_{(5)}} & 0 \\ 0 & 0 & \frac{1}{\alpha^3_{(3)}} & \frac{\varepsilon}{\alpha^4_{(4)}} & 0 & 0 \\ 0 & \frac{1}{\alpha^2_{(2)}} & \frac{\varepsilon}{\alpha^3_{(3)}} & 0 & 0 & 0 \\ \frac{1}{\alpha_{(1)}} & 0 & 0 & 0 & 0 & 0 \end{bmatrix}, \tag{B.13}$$

$$\mathbf{Q}_3 = \begin{bmatrix} 0 & 0 & 0 & 0 & 0 & \alpha_{(1)} \\ 0 & 0 & 0 & 0 & \alpha & 0 \\ \frac{\alpha^3_{(3)}}{\varepsilon^2} & 0 & 0 & 0 & \frac{\alpha^3_{(3)}}{\varepsilon} & -\frac{\alpha^3_{(3)}}{\varepsilon^2} \\ -\frac{\alpha^4_{(4)}}{\varepsilon^3} & 0 & 0 & \frac{\alpha^4_{(4)}}{\varepsilon} & -\frac{\alpha^4_{(4)}}{\varepsilon^2} & \frac{\alpha^4_{(4)}}{\varepsilon^3} \\ \frac{\alpha^5_{(5)}}{\varepsilon^4} & 0 & \frac{\alpha^5_{(5)}}{\varepsilon} & -\frac{\alpha^5_{(5)}}{\varepsilon^2} & \frac{\alpha^5_{(5)}}{\varepsilon^3} & -\frac{\alpha^5_{(5)}}{\varepsilon^4} \\ -\frac{\alpha^6_{(6)}}{\varepsilon^5} & \frac{\alpha^6_{(6)}}{\varepsilon} & -\frac{\alpha^6_{(6)}}{\varepsilon^2} & \frac{\alpha^6_{(6)}}{\varepsilon^3} & -\frac{\alpha^6_{(6)}}{\varepsilon^4} & \frac{\alpha^6_{(6)}}{\varepsilon^5} \end{bmatrix}, \quad \mathbf{Q}_3^{-1} = \begin{bmatrix} \frac{1}{\alpha_{(1)}} & -\frac{\varepsilon}{\alpha^2_{(2)}} & \frac{\varepsilon^2}{\alpha^3_{(3)}} & 0 & 0 & 0 \\ 0 & 0 & 0 & 0 & \frac{1}{\alpha^5_{(5)}} & \frac{\varepsilon}{\alpha^6_{(6)}} \\ 0 & 0 & 0 & \frac{1}{\alpha^4_{(4)}} & \frac{\varepsilon}{\alpha^5_{(5)}} & 0 \\ 0 & 0 & \frac{1}{\alpha^3_{(3)}} & \frac{\varepsilon}{\alpha^4_{(4)}} & 0 & 0 \\ 0 & \frac{1}{\alpha^2_{(2)}} & 0 & 0 & 0 & 0 \\ \frac{1}{\alpha_{(1)}} & 0 & 0 & 0 & 0 & 0 \end{bmatrix}, \tag{B.14}$$

$$\mathbf{Q}_4 = \begin{bmatrix} 0 & 0 & 0 & 0 & 0 & \alpha_{(1)} \\ 0 & 0 & 0 & 0 & \alpha & 0 \\ 0 & 0 & 0 & \alpha^3_{(3)} & 0 & 0 \\ -\frac{\alpha^4_{(4)}}{\varepsilon^3} & 0 & 0 & \frac{\alpha^4_{(4)}}{\varepsilon} & -\frac{\alpha^4_{(4)}}{\varepsilon^2} & \frac{\alpha^4_{(4)}}{\varepsilon^3} \\ \frac{\alpha^5_{(5)}}{\varepsilon^4} & 0 & \frac{\alpha^5_{(5)}}{\varepsilon} & -\frac{\alpha^5_{(5)}}{\varepsilon^2} & \frac{\alpha^5_{(5)}}{\varepsilon^3} & -\frac{\alpha^5_{(5)}}{\varepsilon^4} \\ -\frac{\alpha^6_{(6)}}{\varepsilon^5} & \frac{\alpha^6_{(6)}}{\varepsilon} & -\frac{\alpha^6_{(6)}}{\varepsilon^2} & \frac{\alpha^6_{(6)}}{\varepsilon^3} & -\frac{\alpha^6_{(6)}}{\varepsilon^4} & \frac{\alpha^6_{(6)}}{\varepsilon^5} \end{bmatrix}, \quad \mathbf{Q}_4^{-1} = \begin{bmatrix} \frac{1}{\alpha_{(1)}} & -\frac{\varepsilon}{\alpha^2_{(2)}} & \frac{\varepsilon^2}{\alpha^3_{(3)}} & -\frac{\varepsilon^3}{\alpha^4_{(4)}} & 0 & 0 \\ 0 & 0 & 0 & 0 & \frac{1}{\alpha^5_{(5)}} & \frac{\varepsilon}{\alpha^6_{(6)}} \\ 0 & 0 & 0 & \frac{1}{\alpha^4_{(4)}} & \frac{\varepsilon}{\alpha^5_{(5)}} & 0 \\ 0 & 0 & \frac{1}{\alpha^3_{(3)}} & 0 & 0 & 0 \\ 0 & \frac{1}{\alpha^2_{(2)}} & 0 & 0 & 0 & 0 \\ \frac{1}{\alpha_{(1)}} & 0 & 0 & 0 & 0 & 0 \end{bmatrix}, \tag{B.15}$$

$$\mathbf{Q}_5 = \begin{bmatrix} 0 & 0 & 0 & 0 & 0 & \alpha_{(1)} \\ 0 & 0 & 0 & 0 & \alpha & 0 \\ 0 & 0 & 0 & \alpha^3_{(3)} & 0 & 0 \\ 0 & 0 & \alpha^4_{(4)} & 0 & 0 & 0 \\ \frac{\alpha^5_{(5)}}{\varepsilon^4} & 0 & \frac{\alpha^5_{(5)}}{\varepsilon} & -\frac{\alpha^5_{(5)}}{\varepsilon^2} & \frac{\alpha^5_{(5)}}{\varepsilon^3} & -\frac{\alpha^5_{(5)}}{\varepsilon^4} \\ -\frac{\alpha^6_{(6)}}{\varepsilon^5} & \frac{\alpha^6_{(6)}}{\varepsilon} & -\frac{\alpha^6_{(6)}}{\varepsilon^2} & \frac{\alpha^6_{(6)}}{\varepsilon^3} & -\frac{\alpha^6_{(6)}}{\varepsilon^4} & \frac{\alpha^6_{(6)}}{\varepsilon^5} \end{bmatrix}, \quad \mathbf{Q}_5^{-1} = \begin{bmatrix} \frac{1}{\alpha_{(1)}} & -\frac{\varepsilon}{\alpha^2_{(2)}} & \frac{\varepsilon^2}{\alpha^3_{(3)}} & -\frac{\varepsilon^3}{\alpha^4_{(4)}} & \frac{\varepsilon^4}{\alpha^5_{(5)}} & 0 \\ 0 & 0 & 0 & 0 & \frac{1}{\alpha^5_{(5)}} & \frac{\varepsilon}{\alpha^6_{(6)}} \\ 0 & 0 & 0 & \frac{1}{\alpha^4_{(4)}} & 0 & 0 \\ 0 & 0 & \frac{1}{\alpha^3_{(3)}} & 0 & 0 & 0 \\ 0 & \frac{1}{\alpha^2_{(2)}} & 0 & 0 & 0 & 0 \\ \frac{1}{\alpha_{(1)}} & 0 & 0 & 0 & 0 & 0 \end{bmatrix}, \tag{B.16}$$

$$\mathbf{Q}_6 = \begin{bmatrix} 0 & 0 & 0 & 0 & 0 & \alpha_{(1)} \\ 0 & 0 & 0 & 0 & \alpha & 0 \\ 0 & 0 & 0 & \alpha^3_{(3)} & 0 & 0 \\ 0 & 0 & \alpha^4_{(4)} & 0 & 0 & 0 \\ 0 & \alpha^5_{(5)} & 0 & 0 & 0 & 0 \\ -\frac{\alpha^6_{(6)}}{\varepsilon^5} & \frac{\alpha^6_{(6)}}{\varepsilon} & -\frac{\alpha^6_{(6)}}{\varepsilon^2} & \frac{\alpha^6_{(6)}}{\varepsilon^3} & -\frac{\alpha^6_{(6)}}{\varepsilon^4} & \frac{\alpha^6_{(6)}}{\varepsilon^5} \end{bmatrix}, \quad \mathbf{Q}_6^{-1} = \begin{bmatrix} \frac{1}{\alpha_{(1)}} & -\frac{\varepsilon}{\alpha^2_{(2)}} & \frac{\varepsilon^2}{\alpha^3_{(3)}} & -\frac{\varepsilon^3}{\alpha^4_{(4)}} & \frac{\varepsilon^4}{\alpha^5_{(5)}} & -\frac{\varepsilon^5}{\alpha^6_{(6)}} \\ 0 & 0 & 0 & 0 & \frac{1}{\alpha^5_{(5)}} & 0 \\ 0 & 0 & 0 & \frac{1}{\alpha^4_{(4)}} & 0 & 0 \\ 0 & 0 & \frac{1}{\alpha^3_{(3)}} & 0 & 0 & 0 \\ 0 & \frac{1}{\alpha^2_{(2)}} & 0 & 0 & 0 & 0 \\ \frac{1}{\alpha_{(1)}} & 0 & 0 & 0 & 0 & 0 \end{bmatrix}. \tag{B.17}$$

Appendix C. Calculation of $x_{n+1}(t)$ with one ε-perturbed inactivation rate

Appendix C.1. Constant stimulus, derivation of Eq. (19)

We solve the differential equation (18) through an integrating factor to get:

$$e^{(\beta+\varepsilon)t}x_{n+1}(t) = \alpha_{n+1}\left(\frac{\alpha_{(n)}}{\beta}\right)^n \int e^{(\beta+\varepsilon)t}\mathrm{P}(n,\beta t)\mathrm{d}t + c. \tag{C.1}$$

Use the properties of the Gamma function to re-express the integral as

$$\int e^{(\beta+\varepsilon)t}\mathrm{P}(n,\beta t)\mathrm{d}t = \int e^{(\beta+\varepsilon)t}\mathrm{d}t - \int e^{\varepsilon t}\sum_{k=0}^{n-1}\frac{(\beta t)^k}{k!}\mathrm{d}t. \tag{C.2}$$

and solve the second integral of (C.2) using integration by parts:

$$\int e^{\varepsilon t}\sum_{k=0}^{n-1}\frac{(\beta t)^k}{k!}\mathrm{d}t = \frac{e^{\varepsilon t}}{\varepsilon}\sum_{k=0}^{n-1}\frac{(\beta t)^k}{k!} - \int \frac{\beta e^{\varepsilon t}}{\varepsilon}\left(\sum_{k=0}^{n-1}\frac{(\beta t)^k}{k!} - \frac{(\beta t)^{n-1}}{(n-1)!}\right)\mathrm{d}t \tag{C.3}$$

to obtain

$$\left(1+\frac{\beta}{\varepsilon}\right)\int e^{\varepsilon t}\sum_{k=0}^{n-1}\frac{(\beta t)^k}{k!}\mathrm{d}t=\frac{e^{\varepsilon t}}{\varepsilon}\sum_{k=0}^{n-1}\frac{(\beta t)^k}{k!}+\frac{\beta^n}{\varepsilon(n-1)!}\int e^{\varepsilon t}t^{n-1}\mathrm{d}t. \quad \text{(C.4)}$$

The integral on the right-hand side of equation (C.4) can be solved using the formula [11]:

$$\int e^{\varepsilon t}t^{n-1}\mathrm{d}t=e^{\varepsilon t}\left(\sum_{k=0}^{n-1}\frac{(-1)^k(n-1)!}{\varepsilon^{k+1}(n-1-k)!}t^{n-1-k}\right). \quad \text{(C.5)}$$

Substituting in equation (C.2) and gathering terms we obtain

$$\int e^{(\beta+\varepsilon)t}\mathrm{P}(n,\beta t)\mathrm{d}t=\frac{e^{\varepsilon t}}{\beta+\varepsilon}\left(e^{\beta t}-\sum_{k=0}^{n-1}\frac{(\beta t)^k}{k!}+\frac{(-1)^k\beta^n t^{n-1-k}}{\varepsilon^{k+1}(n-1-k)!}\right)+c, \quad \text{(C.6)}$$

whence Eq. (C.1) becomes

$$x_{n+1}(t)=\frac{\alpha_{n+1}}{\beta+\varepsilon}\left(\frac{\alpha_{(n)}}{\beta}\right)^n\left(1-e^{-\beta t}\sum_{k=0}^{n-1}\left[\frac{(\beta t)^k}{k!}+\frac{(-1)^k\beta^n t^{n-1-k}}{\varepsilon^{k+1}(n-1-k)!}\right]\right)+ce^{-(\beta+\varepsilon)t}. \quad \text{(C.7)}$$

The initial condition $x_{n+1}(0)=0$ requires that

$$c=(-1)^{n+1}\frac{\alpha_{n+1}}{\beta+\varepsilon}\left(\frac{\alpha_{(n)}}{\varepsilon}\right)^n, \quad \text{(C.8)}$$

which gives the final expression given in Eq. (19):

$$x_{n+1}(t)=\frac{\alpha_{n+1}}{\beta+\varepsilon}\left(\frac{\alpha_{(n)}}{\beta}\right)^n\left(1-e^{-\beta t}\left[\left(\frac{-\beta}{\varepsilon}\right)^n e^{-\varepsilon t}+\sum_{k=0}^{n-1}\frac{(\varepsilon^{n-k}-(-\beta)^{n-k})(\beta t)^k}{\varepsilon^{n-k}k!}\right]\right). \quad \text{(C.9)}$$

Appendix C.2. Exponentially decaying stimulus, derivation of Eqs. (21) and (23)

Consider first the case $\beta\neq\lambda$. To solve the differential equation (20), define $\sigma=\beta-\lambda$ and use integrating factors to get:

$$e^{(\beta+\varepsilon)t}x_{n+1}=\alpha_{n+1}\left(\frac{\alpha_{(n)}}{\sigma}\right)^n\left(\int e^{(\sigma+\varepsilon)t}\mathrm{d}t-\int e^{-\varepsilon t}\sum_{k=0}^{n-1}\frac{(\sigma t)^k}{k!}\mathrm{d}t\right)+c. \quad \text{(C.10)}$$

Using integration by parts for the second integral on the right-hand side, and following similar steps to those above gives

$$e^{(\beta+\varepsilon)t}x_{n+1} = \frac{\alpha_{n+1}}{\sigma+\varepsilon}\left(\frac{\alpha_{(n)}}{\sigma}\right)^n\left(e^{(\sigma+\varepsilon)t} - e^{\varepsilon t}\sum_{k=0}^{n-1}\frac{(\varepsilon^{n-k}-(-\sigma)^{n-k})(\sigma t)^k}{\varepsilon^{n-k}k!}\right) + c. \tag{C.11}$$

The initial condition $x_{n+1}(0) = 0$ requires that

$$c = \frac{\alpha_{n+1}}{\sigma+\varepsilon}\left(\frac{\alpha_{(n)}}{\varepsilon}\right)^n, \tag{C.12}$$

thus giving equation (21):

$$x_{n+1}(t) = \frac{\alpha_{n+1}}{\beta+\varepsilon-\lambda}\left(\frac{\alpha_{(n)}}{\beta-\lambda}\right)^n\left[e^{-\lambda t} + \frac{e^{-(\beta+\varepsilon)t}}{\varepsilon^n} - \right.$$
$$\left. - e^{-\beta t}\sum_{k=0}^{n-1}\frac{\left(\varepsilon^{n-k}-(\lambda-\beta)^{n-k}\right)(\beta-\lambda)^k t^k}{\varepsilon^{n-k}k!}\right]. \tag{C.13}$$

When $\lambda = \beta$ we use integrating factors to solve equation (22):

$$x_{n+1}(t)e^{(\beta+\varepsilon)t} = \frac{\alpha_{(n+1)}}{\Gamma(n+1)}\int t^n e^{\varepsilon t}\mathrm{d}t + c \quad = \frac{\alpha_{(n+1)}}{\Gamma(n+1)}\frac{n!}{\varepsilon}\sum_{k=0}^{n}\frac{(-1)^k t^{(n-k)}}{\varepsilon^k(n-k)!} + c, \tag{C.14}$$

and taking the initial condition $x_{n+1}(0) = 0$ we get Eq. (23):

$$x_{n+1}(t) = \left(\frac{\alpha_{(n+1)}}{\varepsilon}\right)^{n+1} e^{-\beta t}\left[\varepsilon^n\sum_{k=0}^{n}\frac{(-1)^k t^{n-k}}{\varepsilon^k(n-k)!} + (-1)^{n+1}e^{-\varepsilon t}\right].$$

Appendix D. Parameter fitting

We use an evolutionary Monte-Carlo optimisation method with local search acceleration to fit the parameters of our models to 'observed data' in Examples 3 and 5. The error function to be minimised is a quadratic distance (sum of squared errors) between the data and the fitted values. In all the fits, the optimisation algorithm was run starting from an initial prior distribution $U(0, 10)$ for each parameter and the algorithm was run for 10 iterations sampling 500 points at each iteration and keeping the best 50 points as a prior for the next iteration. The method is described in detail in Ref. [3].

References

[1] M. Abramowitz and I. A. Stegun, *Handbook of Mathematical Functions with Formulas, Graphs, and Mathematical Tables*, Dover, New York, 9 ed., 1964.

[2] R. L. Bar-Or, R. Maya, L. A. Segel, U. Alon, A. J. Levine, and M. Oren, *Generation of oscillations by the p53-Mdm2 feedback loop: a theoretical and experimental study.*, Proc Natl Acad Sci USA, 97 (2000), pp. 11250–11255.

[3] M. Beguerisse-Díaz, B. Wang, R. Desikan, and M. Barahona, *Squeeze-and-Breathe Evolutionary Monte Carlo Optimisation with Local Search Acceleration and its application to parameter fitting*, arXiv:1107.2879, (2011).

[4] R. Bellman, R. Bellman, and K. Cooke, *Differential-difference equations*, Mathematics in science and engineering, Academic Press, 1963.

[5] S. Bernard, B. Cajavec, L. Pujo-Menjouet, M. C. Mackey, and H. Herzel, *Modelling transcriptional feedback loops: the role of Gro/TLE1 in Hes1 oscillations.*, Philosophical Transactions of the Royal Society of London. Series A: Physical and Engineering Sciences, 364 (2006), pp. 1155–1170.

[6] L. Chang and M. Karin, *Mammalian MAP kinase signalling cascades.*, Nature, 410 (2001), pp. 37–40.

[7] M. Chaves, E. D. Sontag, and R. J. Dinerstein, *Optimal Length and Signal Amplification in Weakly Activated Signal Transduction Cascades*, The Journal of Physical Chemistry B, 108 (2004), pp. 15311–15320.

[8] C. Colijn and M. C. Mackey, *A mathematical model of hematopoiesis–I. Periodic chronic myelogenous leukemia.*, Journal of Theoretical Biology, 237 (2005), pp. 117–132.

[9] E. Feliu, L. N. Andersen, M. Knudsen, and C. Wiuf, *A General Mathematical Framework Suitable for Studying Signaling Cascades*, arXiv:1008.0427, (2010).

[10] S. Friedberg, A. Insel, and L. Spence, *Linear algebra*, Pearson Education, 2003.

[11] I. Gradshteyn and I. Ryzhik, *Table of Integrals, Series, and Products*, Academic Press, 2007.

[12] R. Heinrich, B. G. Neel, and T. A. Rapoport, *Mathematical Models of Protein Kinase Signal Transduction*, Molecular Cell, 9 (2002), pp. 957–970.

[13] T. Höfer, H. Nathansen, M. Löhning, A. Radbruch, and R. Heinrich, *GATA-3 transcriptional imprinting in Th2 lymphocytes: a mathematical model.*, Proc Natl Acad Sci USA, 99 (2002), pp. 9364–9368.

[14] S. Hooshangi, S. Thiberge, and R. Weiss, *Ultrasensitivity and noise propagation in a synthetic transcriptional cascade*, Proc Natl Acad Sci USA, 102 (2005), pp. 3581–3586.

[15] C. Y. Huang and J. E. Ferrell, *Ultrasensitivity in the mitogen-activated protein kinase cascade*, Proc Natl Acad Sci USA, 93 (1996), pp. 10078–10083.

[16] B. N. Kholodenko, *Negative feedback and ultrasensitivity can bring about oscillations in the mitogen-activated protein kinase cascades.*, Eur J Biochem, 267 (2000), pp. 1583–1588.

[17] A. L. Lucius, N. K. Maluf, C. J. Fischer, and T. M. Lohman, *General Methods for Analysis of Sequential n-step Kinetic Mechanisms: Application to Single Turnover Kinetics of Helicase-Catalyzed DNA Unwinding*, Biophysical Journal, 85 (2003), pp. 2224–2239.

[18] F. Marks, U. Klingmüller, and K. Müller-Decker, *Cellular signal processing: an introduction to the molecular mechanisms of signal transduction*, Garland Science, 2009.

[19] N. A. M. Monk, *Oscillatory expression of Hes1, p53, and NF-kappaB driven by transcriptional time delays.*, Current Biology, 13 (2003), pp. 1409–1413.

[20] R. B. Paris, *Incomplete Gamma and Related Functions*, in NIST Digital Library of Mathematical Functions, 2010.

[21] J. Stark, C. Chan, and A. J. T. George, *Oscillations in the immune system*, Immunological Reviews, 216 (2007), pp. 213–231.

[22] J. Stricker, S. Cookson, M. R. Bennett, W. H. Mather, L. S. Tsimring, and J. Hasty, *A fast, robust and tunable synthetic gene oscillator.*, Nature, 456 (2008), pp. 516–519.

[23] J. J. Tyson, K. C. Chen, and B. Novak, *Sniffers, buzzers, toggles and blinkers: dynamics of regulatory and signaling pathways in the cell*, Current Opinion in Cell Biology, 15 (2003), pp. 221 – 231.

[24] B. Wang, R. I. Kitney, N. Joly, and M. Buck, *Engineering modular and orthogonal genetic logic gates for robust digital-like synthetic biology.*, Nat Commun, 2 (2011), p. 508.

[25] S. Yi and A. Ulsoy, *Solution of a system of linear delay differential equations using the matrix Lambert function*, in American Control Conference, 2006, june 2006, p. 6 pp.

[26] S. Zhang and D. F. Klessig, *MAPK cascades in plant defense signaling*, Trends Plant Sci, 6 (2001), pp. 520–527.